

**PHOTOINDUCED ELECTRON-TRANSFER REACTIONS BETWEEN
C₆₀ AND CYCLIC DISILIRANES (c-R₂Si-X-SiR₂; X = SiR₂, CH₂, O,
NPh, S)**

Yoshiko Sasaki,^a Mamoru Fujitsuka,^b Osamu Ito,^{*b} Yutaka Maeda,^c Takatsugu Wakahara,^c Takeshi Akasaka,^c Kaoru Kobayashi,^d Shigeru Nagase,^d Masahiro Kako,^e and Yasuhiro Nakadaira^e

^aShokei Girls' High School, Hirose-machi, Aoba-ku, Sendai, 980-0873, Japan,

^bInstitute for Chemical Reaction Science, Tohoku University, Katahira, Aoba-ku, Sendai 980-8577, Japan, ^cGraduate School of Science and Technology, Niigata

University, Niigata 950-2181, Japan, ^dDepartment of Chemistry, Graduate School of Science, Tokyo Metropolitan University, Hachioji, Tokyo 192-0397, Japan,

^eDepartment of Applied Physics and Chemistry, The University of Electro-Communications, Tokyo 182-8585, Japan

Abstract - Photoinduced electron-transfer reactions between various cyclic disiliranes (c-R₂Si-X-SiR₂; X = SiR₂, CH₂, O, NPh, and S) and photo-excited C₆₀ in polar PhCN solvent have been investigated by 532 nm laser photolysis with the observation of the transient absorption bands in the near-IR region. The transient absorption band of the anion radical of C₆₀ (C₆₀^{•-}) appeared at 1070 nm, accompanying the decay of the excited triplet state of C₆₀ (³C₆₀^{*}), showing that electron transfer takes place from c-R₂Si-X-SiR₂ to ³C₆₀^{*}. The rates and quantum yields for electron transfer *via* ³C₆₀^{*} were compared with changing X. The final products in PhCN were identified as mono-adducts and bis-adducts of R₂Si-X-SiR₂ with PhCN, but not with C₆₀^{•-}.

Email: ito@icrs.tohoku.ac.jp FAX: +81 22 217 5608

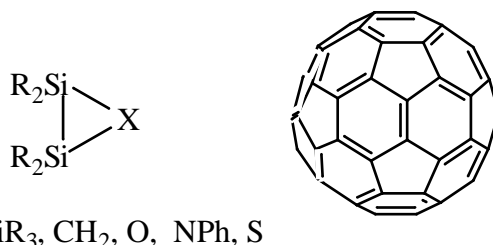
This study is dedicated to Professor Sho Ito.

INTRODUCTION

Photoreactions of C_{60} have been studied extensively to functionalize C_{60} .¹⁻⁵ The mechanism for the photoinduced reactions has been revealed by direct methods observing the transient absorption bands of both excited state of C_{60} and ion radicals of C_{60} in the near-IR region.⁶⁻¹¹ In appropriately concentration of electron donors, electron transfer tends to take place *via* the triplet excited state of C_{60} ($^3C_{60}^*$) in polar solvents as shown by the nano-second time-resolved spectroscopy.⁶⁻⁹ Since the intersystem crossing rate of C_{60} is as fast as 10^9 s⁻¹,⁹ electron transfer *via* the singlet excited state of C_{60} ($^1C_{60}^*$) takes place only when the electron-donors are more than a few mol dm⁻³ in polar and non-polar solvents.^{10,11}

In the previous studies, it has been reported that cyclic disiliranes ($c\text{-R}_2\text{Si-CH}_2\text{-SiR}_2$) act as good electron donors toward photoexcited C_{60} .¹²⁻¹⁵ In usual solvents, which do not react with the cation radical of $c\text{-R}_2\text{Si-CH}_2\text{-SiR}_2$ [$(c\text{-R}_2\text{Si-CH}_2\text{-SiR}_2)^{\bullet+}$], the cycloadducts between C_{60} and $(c\text{-R}_2\text{Si-CH}_2\text{-SiR}_2)^{\bullet+}$ were produced. On the other hand, in PhCN and in Ph₂C=O, $(c\text{-R}_2\text{Si-CH}_2\text{-SiR}_2)^{\bullet+}$ reacts after ring-opening with PhCN and Ph₂C=O, yielding mono-adducts and bis-adducts.¹⁴

In the present study, we examined the electron-donor abilities of various cyclic disiliranes ($c\text{-R}_2\text{Si-X-SiR}_2$; X=CH₂, O, S, NPh, and SiR₂) to photo-excited C_{60} in polar PhCN (Scheme 1).



Scheme 1

The observed efficiencies and rate constants for electron transfer *via* $^3C_{60}^*$ are compared among $c\text{-R}_2\text{Si-X-SiR}_2$. The order of electron-donor abilities is compared with the free-energy changes calculated from the oxidation potentials of $c\text{-R}_2\text{Si-X-SiR}_2$. Some MO considerations are also performed to interpret the observed electron-donor abilities of $(c\text{-R}_2\text{Si-X-SiR}_2)$.¹⁶

RESULTS AND DISCUSSION

Steady-state UV/Visible spectra

The steady-state absorption spectra of $c\text{-R}_2\text{Si-S-SiR}_2$, C_{60} and their mixture in PhCN are shown in Figure 1, in which $c\text{-R}_2\text{Si-S-SiR}_2$ has no absorption in the longer wavelength region than 400 nm. The absorption spectrum of a mixture of C_{60} and $c\text{-R}_2\text{Si-S-SiR}_2$ in PhCN is almost same as that of C_{60} in the

longer wavelength region than 600 nm. In the region of 400 - 600 nm, the absorption of the mixture is slightly stronger than that of C₆₀, suggesting that there is a weak interaction between C₆₀ and c-R₂Si-S-SiR₂ in the ground states. The laser-photolysis experiments were performed under the concentration conditions shown in the caption of Figure 1, showing such quite weak interaction between C₆₀ and c-R₂Si-S-SiR₂. The laser light at 532 nm predominantly excites C₆₀. For other C₆₀/c-R₂Si-X-SiR₂ systems, spectral features similar to that of C₆₀/c-R₂Si-S-SiR₂ were observed.

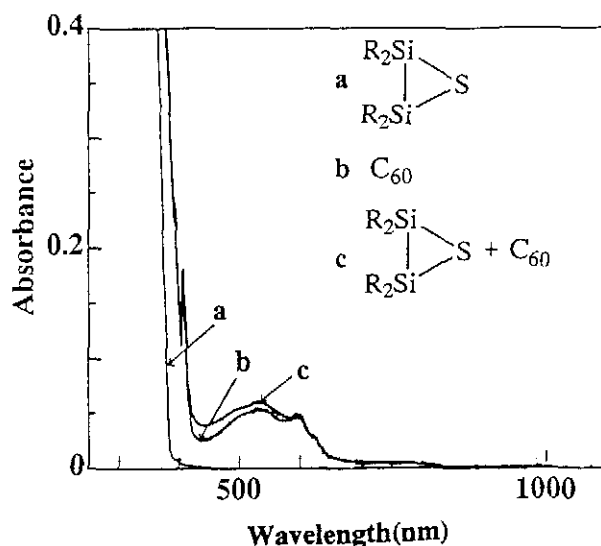


Figure 1. Steady-absorption spectra of (a) c-R₂Si-S-SiR₂ (2×10^{-3} mol dm⁻³), (b) C₆₀ (0.1×10^{-3} mol dm⁻³), and (c) their mixture in PhCN.

Transient spectra in PhCN.

The transient absorption spectra obtained by 532 nm laser photolysis of C₆₀ (0.1×10^{-3} mol dm⁻³) in the presence of c-R₂Si-N(Ph)-SiR₂ (2.0×10^{-3} mol dm⁻³) in PhCN are shown Figure 2. The absorption band of ³C₆₀* at 740 nm,⁶⁻⁹ which appeared immediately after the laser exposure, began to decay in the presence of c-R₂Si-N(Ph)-SiR₂. Accompanied by the decay of ³C₆₀*, the absorption intensity of C₆₀*⁻ at 1070 nm increased, which suggests that electron transfer for the C₆₀*⁻ formation takes place *via* ³C₆₀*, accepting an electron from c-R₂Si-N(Ph)-SiR₂ (Scheme 2). For other C₆₀/c-R₂Si-X-SiR₂, similar transient spectra were observed.

The time profiles for the decay of ³C₆₀* at 740 nm and rise of C₆₀*⁻ at 1070 nm are shown in inset of Figure 2 in the case of C₆₀/c-R₂Si-N(Ph)-SiR₂. The decay curve of ³C₆₀* and rise curve of C₆₀*⁻ are almost mirror image, supporting the electron-transfer mechanism shown in Scheme 2.

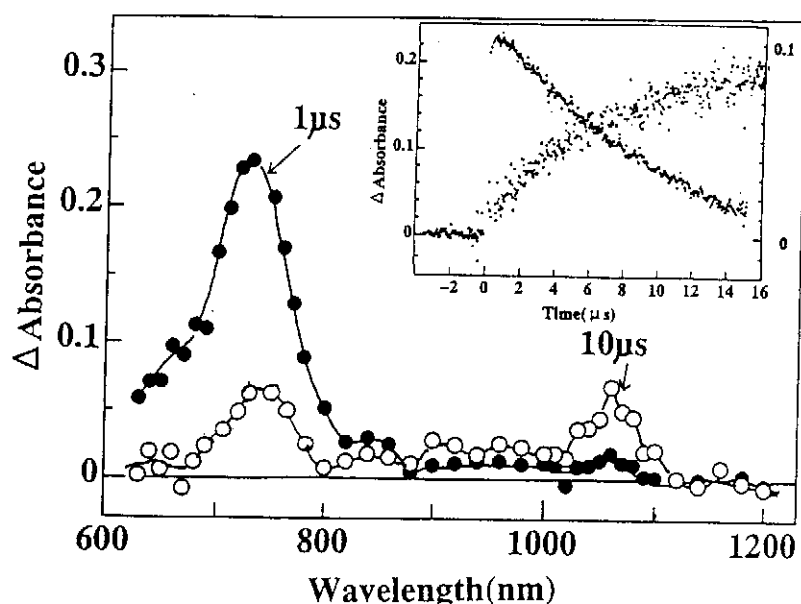
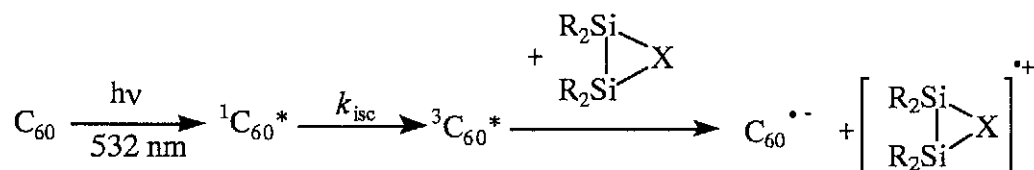


Figure 2. Transient absorption spectra observed by 532 nm-laser flash photolysis of C_{60} ($0.1 \times 10^{-3} \text{ mol dm}^{-3}$) in the presence of $c\text{-R}_2\text{Si-N(Ph)-SiR}_2$ ($2 \times 10^{-3} \text{ mol dm}^{-3}$) in deaerated PhCN. Inset: Time profiles at 740 and 1070 nm for C_{60} ($0.1 \times 10^{-3} \text{ mol dm}^{-3}$) and $c\text{-R}_2\text{Si-S-SiR}_2$ ($2 \times 10^{-3} \text{ mol dm}^{-3}$) in deaerated PhCN.



Scheme 2; in polar solvents

The decay of ${}^3C_{60}^*$ at 740 nm and rise of $C_{60}^{\bullet-}$ at 1070 nm obey first-order kinetics, yielding the first-order rate constant (k_{1st}). The k_{1st} values increase with the concentration of $c\text{-R}_2\text{Si-X-SiR}_2$. The second-order rate constant (k_q) can be obtained from the slope of the pseudo-first-order plots as listed in Table 1.

From the ratio of the initial absorbance at 740 nm to the saturated absorbance at 1070 nm, the efficiency of electron transfer *via* ${}^3C_{60}^*$ can be obtained. At sufficiently high concentration of $c\text{-R}_2\text{Si-X-SiR}_2$ up to *ca.* $5 \times 10^{-3} \text{ mol dm}^{-3}$, the efficiency can be put equal to the quantum yield (Φ_{et}) of the electron transfer process *via* ${}^3C_{60}^*$ as shown in the following relation (A and ϵ refer to absorbance and molar extinction coefficient, respectively).^{17,18}

$$\Phi_{et} = [C_{60}^{\bullet-}] / [{}^3C_{60}^*] = (A_{1070 \text{ nm}} / A_{740 \text{ nm}}) / (\epsilon_{740 \text{ nm}} / \epsilon_{1070 \text{ nm}}) \quad (\text{eq 1})$$

Table 1. HOMO levels, oxidation potentials (E_{ox}), free-energy changes (ΔG°_{et}) for electron transfer, rate constants for quenching (k_q) of ${}^3C_{60}^*$, quantum yield (Φ_{et}) and rate constant (k_{et}) for electron-transfer via ${}^3C_{60}^*$ in PhCN.

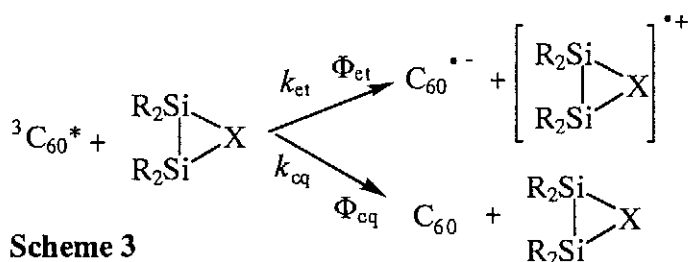
X in c-R ₂ Si-X-SiR ₂	HOMO eV	E _{ox} ^c V	ΔG°_{et} kcal/mol	k_q mol ⁻¹ dm ³ s ⁻¹	Φ_{et}	k_{et} mol ⁻¹ dm ³ s ⁻¹	Product mono % bis %	
>Si(R ₂) ^a	-7.90	0.76	-8.65	1.4 x 10 ⁹	0.50	7.0 x 10 ⁸	0	0
>CH ₂ ^a	-7.58	0.81	-7.49	2.0 x 10 ⁸	0.67	1.3 x 10 ⁸	51	18
>O ^b	-7.17	0.97	-3.80	1.5 x 10 ⁸	0.78	1.2 x 10 ⁸	62	0
>N(Ph) ^a	-7.70	0.99	-3.34	2.1 x 10 ⁸	0.32	6.8 x 10 ⁷	— ^d	
>S ^a	-8.07	1.01	-2.88	1.2 x 10 ⁸	0.30	3.7 x 10 ⁷	30	

^a R = Mesityl. ^b R = Diethylphenyl.

^c Pt-electrode in CH₂Cl₂ with 0.1 mol dm⁻³ (n-Bu)₄ClO₄.

^d Mono-adduct was identified by a MS analysis.

Thus, the Φ_{et} values were evaluated as listed in Table 1. These Φ_{et} values are all smaller than 1, indicating that the electron-transfer process via ${}^3C_{60}^*$ is in competitive with the other deactivation processes of ${}^3C_{60}^*$ such as collisional deactivation as shown in Scheme 3. Thus, the electron-transfer rate-constant (k_{et}) can be obtained from the relation of $k_{et} = \Phi_{et} k_q$ as listed in Table 1.^{17,18} Thus, the k_{et} values in the order of 10⁷ - 10⁸ mol⁻¹ dm³ s⁻¹ were obtained, which are 10 - 10² less than the diffusion controlled limit ($k_{diff} = 5.2 \times 10^9$ mol⁻¹ dm³ s⁻¹ in PhCN).¹⁹



From the Rehm-Weller equation,²⁰ the free-energy change (ΔG°_{et}) can be calculated for the electron-transfer systems of ${}^3C_{60}^*/c-R_2Si-X-SiR_2$ in PhCN by employing the T₁-energy level of ${}^3C_{60}^*$ (1.50 eV),²¹ the reduction potential of C₆₀ (-0.43 V vs SCE), the oxidation potentials of c-R₂Si-X-SiR₂ (Table 1), and the Coulomb energy (0.06 eV).²¹ The observed k_{et} values are plotted against these ΔG°_{et} as shown in Figure 3, in which the curve was calculated one on the basis of the empirical Rehm-Weller equation.²⁰ The

observed k_{et} value for $c\text{-R}_2\text{Si-X-SiR}_2$ with sufficiently negative ΔG°_{et} would be anticipated to be close to k_{diff} , while on going to positive ΔG°_{et} , the k_{et} value would be anticipated to decrease.²⁰

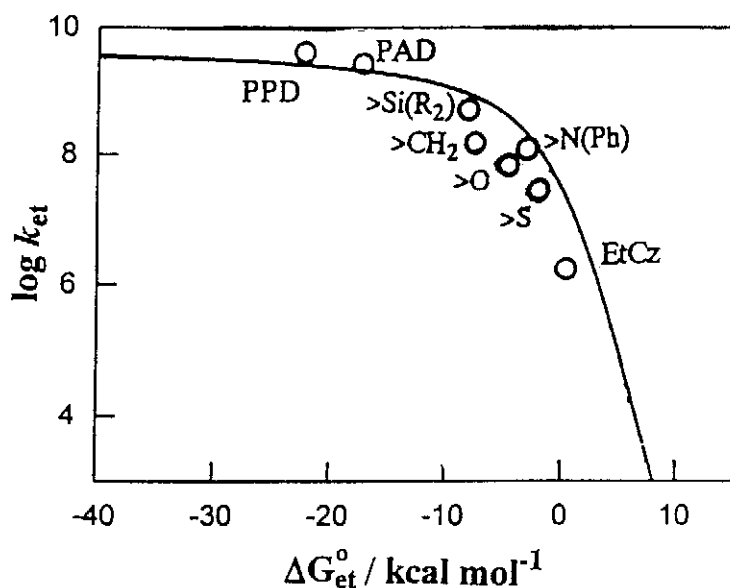


Figure 3. Plots of $\log k_{et}$ vs ΔG°_{et} ; the curve was calculated from Rehm-Weller equation. PAD (*p*-anisidine), PPD (*p*-phenylenediamine), EtCz (ethyl carbazole).

Usually, the ΔG°_{et} values for electron transfer should be calculated using the corresponding E_{ox} values in the same solvent; however, in the case of $c\text{-R}_2\text{Si-X-SiR}_2$, the E_{ox} value of $c\text{-R}_2\text{Si-S-SiR}_2$ is extremely larger than that in CH_2Cl_2 , predicting the k_{et} value as small as $10^4 \text{ mol}^{-1} \text{ dm}^3 \text{ s}^{-1}$ in PhCN from Rehm-Weller curve.²⁰ Thus, we employed the E_{ox} values in CH_2Cl_2 for the calculation of the ΔG°_{et} values in Table 1.

The HOMO-levels of $c\text{-R}_2\text{Si-X-SiR}_2$ calculated from the MO method well predict the electron-donor abilities, excepting $c\text{-R}_2\text{Si-Si(R}_2\text{)-SiR}_2$ and $c\text{-R}_2\text{Si-O-SiR}_2$.¹⁶ Both the observed E_{ox} and k_{et} values indicate that $c\text{-R}_2\text{Si-Si(R}_2\text{)-SiR}_2$ has the highest electron-donor ability in Table 1; however, the calculated HOMO-level of $c\text{-R}_2\text{Si-Si(R}_2\text{)-SiR}_2$ is as low as that of $c\text{-R}_2\text{Si-S-SiR}_2$. The calculated HOMO-level of $c\text{-R}_2\text{Si-O-SiR}_2$ is highest; however, the electron-donor ability is intermediate. Further MO-calculations may be necessary.

Steady-state photolysis

By the repeated irradiation of 532 nm laser light on C_{60} in the presence of $c\text{-R}_2\text{Si-N(Ph)-SiR}_2$ in deaerated PhCN, the absorption spectra changed as shown in Figure 4. The steady-state concentration of the absorption band of C_{60}^{\bullet} appeared at 1070 nm, which increased with time and then decreased.

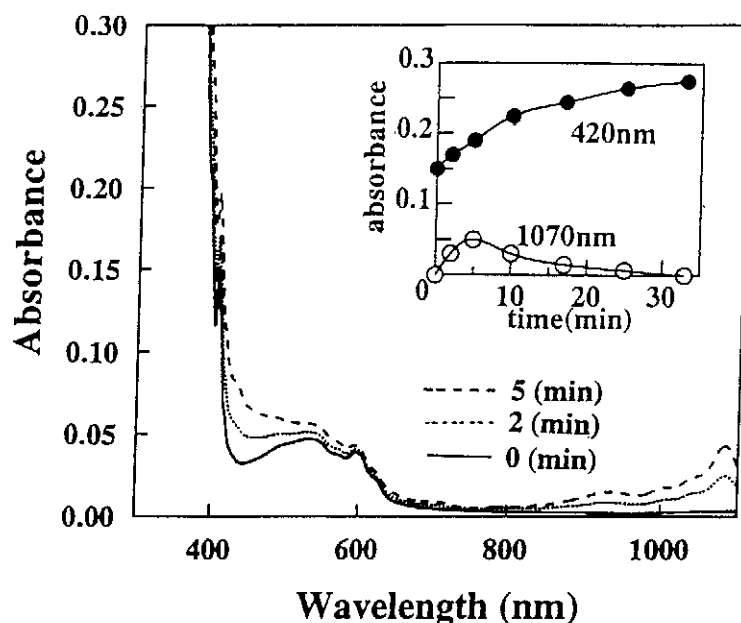


Figure 4. Steady-state absorption spectra observed by 532 nm-laser flash photolysis of C_{60} ($0.1 \times 10^{-3} \text{ mol dm}^{-3}$) in the presence of $c\text{-R}_2\text{Si-N(Ph)-SiR}_2$ ($2 \times 10^{-3} \text{ mol dm}^{-3}$) in deaerated PhCN.

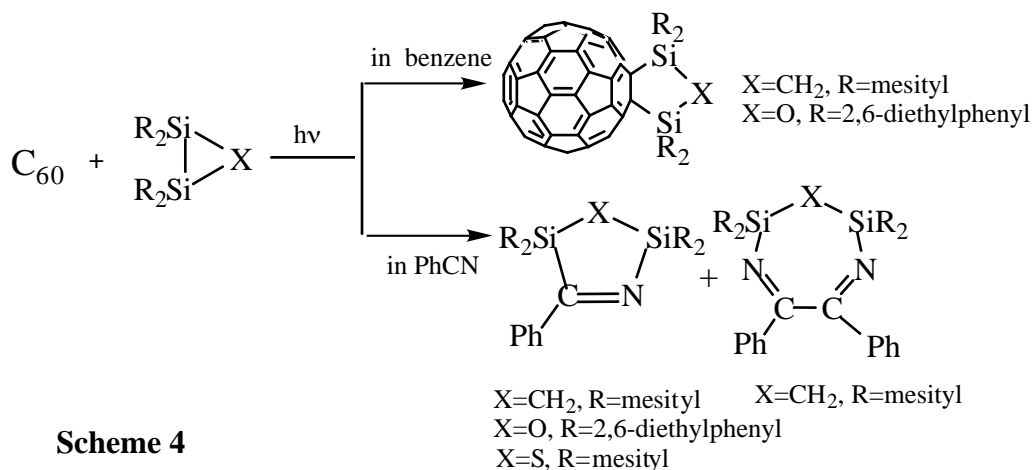
The finding that the steady-concentration of $C_{60}^{\bullet-}$ was observed indicates that the back electron transfer from $C_{60}^{\bullet-}$ to $[c\text{-R}_2\text{Si-X-SiR}_2]^{*+}$ was retarded.²² This implies that $[c\text{-R}_2\text{Si-X-SiR}_2]^{*+}$ changes into the substance with less electron-accepting abilities; i.e., ring opening of $[c\text{-R}_2\text{Si-X-SiR}_2]^{*+}$ separates the radical center and cation center, which have usually less electron-acceptor ability compared with the cation radical of the molecule. After reaching the maximum, $C_{60}^{\bullet-}$ begins to decrease, which suggests that $C_{60}^{\bullet-}$ donates electron to the gradually produced cations and/or radicals of the adducts.

In the region of the absorption of neutral C_{60} , appreciable change in the shape of the absorption bands was not observed. The observed slight spectral change in the visible region suggests that the absorption tails extending from the shorter wavelength region increase. The increase in the 420 nm (inset of Figure 4) may reflect an increase in the absorption tail, but not new adducts between $C_{60}^{\bullet-}$ and $[c\text{-R}_2\text{Si-X-SiR}_2]^{*+}$.

Product analysis

When benzene, toluene, and *o*-dichlorobenzene (*o*-DCB) were used as solvents, the adducts between C_{60} and $c\text{-R}_2\text{Si-X-SiR}_2$ were identified as shown in Scheme 4. In benzene and toluene, no clear electron-transfer process was found by nano-second laser flash photolysis, suggesting that the exciplex may be a reaction intermediate.^{1,14,23}

In PhCN, on the other hand, $C_{60}^{\bullet -}$ and $[c-R_2Si-X-SiR_2]^+$ were separately surrounded by PhCN, decreasing a chance for the reaction of $[c-R_2Si-X-SiR_2]^+$ with $C_{60}^{\bullet -}$, while a chance for the reaction with PhCN increases, yielding mono-adducts and bis-adducts as shown in Scheme 4. In Table 1, some data for the yields of mono-adducts and bis-adducts are listed. Such product analysis experiments are still in progress.



EXPERIMENTAL

C_{60} of 99.99 % purity was obtained from Texas Fullerenes Corp. Cyclic disiliranones ($(c-R_2Si-X-SiR_2)$; $X = CH_2$,²⁴ O ,²⁵ S ,²⁶ NPh ,²⁷ and SiR_2 ²⁸) were prepared by the reported methods. The solutions of C_{60} and disiliranones were deaerated with Ar-bubbling before measurements.

C_{60} in the solution was selectively excited by the laser light at 532 nm from a Nd:YAG laser (6 ns fwhm) with power of 7 mJ. For short-time measurement from 50 ns to 10 μs , a pulsed xenon flash lamp was used as a probe beam, which was detected with a Ge-APD module (Hamamatsu, C5331-SPL) after passing through a photochemical quartz vessel (10 mm x 10 mm) and a monochromator.⁹ For the longer time-scale measurements (> 10 μs), the steady Xe-light (150 W) was employed as a monitor light, which was detected with InGaAs photodiode. The steady-state UV/VIS/near-IR absorption spectra were recorded with a JASCO spectrophotometer. The product analysis was performed by TOF-MS. All experiments were performed at 22 °C. MO calculations were performed at the PM3 level using the Gaussian 98 program.¹⁶

Representative analytical data for adducts are as follows.

For $c-Mes_2Si-CH_2-SiMes_2/C_{60}$ adduct (Mes=mesityl): 1H NMR (500 MHz, $CS_2/CH_2Cl_2=3:1$) δ

6.68(s, 2H) 6.64(s, 2H), 6.50(s, 2H), 6.46(s, 2H), 3.61(d, J=13.0 Hz, 1H), 3.16(s, 6H), 2.90(s, 6H), 2.41(s, 6H), 2.38(d, J=13.0 Hz, 1H), 2.17(s, 6H), 2.13(s, 6H), 2.10(s, 6H); ^{13}C NMR (125M Hz, $\text{CS}_2/\text{H}_2\text{Cl}_2=3:1$) δ (number of carbon atoms on C_{60}) 147.23(2), 146.80(2), 146.51(2), 146.17(12), 145.58(2), 145.34(2), 144.64(2), 144.52(2), 144.40(2), 144.06(2), 143.68(1), 143.57, 143.45(1), 143.10, 143.01, 142.69(2), 142.37, 142.17(4), 142.57(1), 141.69(2), 141.57(5), 141.37(2), 140.95(2), 139.41, 139.10(2), 138.57(2), 138.24, 135.38(2), 133.17, 132.50, 130.82, 130.58(2), 130.21, 129.62, 128.98, 73.36(2), 30.77, 26.69, 26.33, 24.13, 20.95, 10.18(2); ^{29}Si NMR ($\text{CS}_2/\text{CH}_2\text{Cl}_2=3:1$) δ -9.81; FAB MS, m/z 1270 – 1266 ($\text{Mes}_2\text{SiCH}_2\text{SiMes}_2/\text{C}_{60}$), 723 - 720 (C_{60}).

For c- $\text{Mes}_2\text{Si-CH}_2\text{-SiMes}_2/\text{PhCN}$ adduct: $^1\text{H-NMR}$ (500 MHz, CD_2Cl_2) δ 7.24(m, H), 7.15(br s, 2H), 7.14(br s, 2H), 6.55(s, 4H), 6.50(s, 4H), 2.23(s, 12H), 2.17(s, 6H), 2.16(s, 6H), 2.05(s, 12H), 1.61(s, 2H); $^{13}\text{C-NMR}$ (125 MHz, CD_2Cl_2) δ 201.18, 143.60, 143.46, 143.03, 138.45, 137.33, 134.73, 131.51, 129.14*, 128.65, 127.64, 125.89, 24.70, 23.37, 20.31, 20.29, 11.12, *One peak was overlapped. Detected by gradient HMQC; $^{29}\text{Si-NMR}$ (100 MHz, CD_2Cl_2) δ -0.21, -8.25; FT-IR (neat) 1604 cm^{-1} ; UV/VIS (λ_{max} , hexane) 219, 225, 272 nm; FAB MS, m/z 650 (M+H).

For c- $\text{Mes}_2\text{Si-CH}_2\text{-SiMes}_2/(\text{PhCN})_2$ adduct: $^1\text{H-NMR}$ (500 MHz, CD_2Cl_2) δ 7.69(d, J= 7.0 Hz, 4H), 6.86(s, 4H), 6.84(d, J= 7.0 Hz, 2H), 6.76(t, J= 7.0 Hz, 4H), 6.21(s, 4H), 2.96(s, 12H), 2.53(s, 12H), 2.75(s, 6H), 2.13(s, 6H), 2.12(s, 2H); $^{13}\text{C-NMR}$ (125 MHz, CD_2Cl_2) δ 178.78, 144.74, 144.26, 139.09, 138.70, 138.64, 135.28, 133.56, 130.88, 130.27, 129.88, 129.04, 127.99, 25.30, 24.72, 21.46, 21.18, 14.94; $^{29}\text{Si-NMR}$ (100 MHz, CD_2Cl_2) δ -15.98; FT-IR (neat) 1604 cm^{-1} ; UV/VIS (λ_{max} , hexane) 222, 261 nm; FAB MS, m/z 753 (M+H).

For c- $\text{Dep}_2\text{Si-O-SiDep}_2/\text{PhCN}$ adduct (Dep=2,6-diethylphenyl): $^1\text{H-NMR}$ (500 MHz, CD_2Cl_2) δ 7.60(dd, J=2.0, 6.5 Hz, 2H), 7.23-7.38(m, 7H), 7.00(d, J=7.5 Hz, 4H), 6.99(d, J= 7.5 Hz, 4H), 3.07(q, J= 7.3 Hz, 4H), 2.68(q, J= 7.3 Hz, 4H), 2.62(q, J= 7.3 Hz, 4H), 2.43(q, J= 7.3 Hz, 4H), 0.77(t, J= 7.3 Hz, 12H), 0.61(t, J= 7.3 Hz, 12H); $^{13}\text{C-NMR}$ (125 MHz, CD_2Cl_2) δ 201.71, 150.08, 149.13, 145.13, 135.45, 133.08, 129.62, 129.61, 129.03, 127.47, 127.15, 125.93, 125.72, 29.93, 28.32, 15.13, 14.31; $^{29}\text{Si-NMR}$ (100 MHz, CD_2Cl_2) δ -6.38, -19.47; FT-IR (neat) 1587 cm^{-1} ; UV/VIS (λ_{max} , hexane) 213, 239, 253 nm; FAB MS, m/z 708 (M+H).

For c- $\text{Mes}_2\text{Si-S-SiMes}_2/\text{PhCN}$ adduct: yellow oil. $^1\text{H NMR}$ (300 MHz, C_6D_6): δ 8.24 (d, 2H, J = 9 Hz), 7.10-6.98 (m, 3H), 6.68 (s, 4H), 6.62 (s, 4H), 2.67 (s, 12H), 2.36 (s, 12H), 2.04 (s, 6H), 2.02 (s, 6H). ^{13}C NMR (75 MHz, C_6D_6): δ 198.28, 144.40, 144.39, 143.25, 139.83, 139.36, 132.95, 132.12, 130.85, 130.25, 129.98, 129.28, 128.77, 25.66, 24.07, 20.01*. *One peak was overlapped. ^{29}Si NMR (60 MHz,

C₆D₆): δ 11.75, 4.44; FAB MS, m/z 668 (M+H).

ACKNOWLEDGEMENT

This work was partly supported by the Grant-in-Aid on General-Research (No. 11440211) and the Grant-in-Aid of Priority-Area-Research on "Laser Chemistry of Single Nanometer Organic Particle" (No. 10207202) from the Ministry of Education, Science, Sports and Culture.

REFERENCES AND NOTE

- 1 T. Akasaka, W. Ando, K. Kobayashi, and S. Nagase, *J. Am. Chem. Soc.*, 1993, **115**, 10366.
- 2 H. Tokuyama, H. Isobe, and E. Nakamura, *J. Chem. Soc., Chem. Commun.*, 1994, 2753.
- 3 J. Averdung, G. Torres-Garcia, H. Luftmann, I. Schlachter, and J. Mattay, *Full. Science Techn.*, 1996, **4**, 633.
- 4 K. Mikami, S. Matsumoto, A. Ishida, S. Takamuku, T. Suenobu, and S. Fukuzumi, *J. Am. Chem. Soc.*, 1995, **117**, 11134.
- 5 S. Fukuzumi, T. Suenobu, M. Fujitsuka, O. Ito, T. Tonoi, S. Matsumoto, and K. Mikami, *J. Organomet. Chem.*, 1999, **32**, 574.
- 6 O. Ito, Y. Sasaki, A. Watanabe, R. Hoffmann, C. Siedschlag, and J. Mattay, *J. Chem. Soc., Perkin Trans. 2*, 1997, 1007.
- 7 J. W. Arbogast and C. S. Foote, *J. Am. Chem. Soc.*, 1991, **113**, 8886.
- 8 L. Biczok and H. Linschitz, *Chem. Phys. Lett.*, 1992, **195**, 339.
- 9 O. Ito, *Res. Chem. Intermed.*, 1966, **23**, 389.
- 10 R. Sension, A. Z. Szarka, G. R. Smith, and R. M. Hochstrasser, *Chem. Phys. Lett.*, 1991, **185**, 179.
- 11 H. N. Ghosh, H. Pal, A. V. Sapre, and J. P. Mittal, *J. Am. Chem. Soc.*, 1993, **115**, 11722.
- 12 T. Akasaka, W. Ando, K. Kobayashi, and S. Nagase, *J. Am. Chem. Soc.*, 1993, **115**, 10366.
- 13 T. Akasaka, E. Mitsuhida, W. Ando, K. Kobayashi, and S. Nagase, *J. Am. Chem. Soc.*, 1994, **116**, 2627.
- 14 T. Akasaka, Y. Maeda, T. Wakahara, M. Okamura, M. Fujitsuka, O. Ito, K. Kobayashi, S. Nagase, M. Kako, Y. Nakadaira, and E. Horn, *Org. Lett.*, 1999, **1**, 1509.
- 15 Y. Sasaki, T. Konoshi, M. Fujitsuka, O. Ito, Y. Maeda, T. Wakahara, T. Akasaka, M. Kako, Y. Nakadaira, *J. Organomet. Chem.*, 2000, **599**, 216.
- 16 J. J. P. Stewart, *J. Comput. Chem.*, 1989, **10**, 209.
- 17 C. A. Steren, H. von Willigen, L. Biczok, N. Gupta, and H. Linschitz, *J. Phys. Chem.*, 1996, **100**, 8920.
- 18 Y. Sasaki, T. Konishi, M. Fujitsuka, and O. Ito, *Phys. Chem. Chem. Phys.*, 1999, **1**, 4555.
- 19 S. T. Murov, I. Carmichael, and G. L. Hug, *Handbook of Photochemistry*, 2nd Edition, Dekker, New York, 1993.
- 20 D. Rehm and A. Weller, *Isr. J. Chem.*, 1970, **8**, 259.

- 21 J. W. Arbogast, C. S. Foote, and M. Kao, *J. Am. Chem. Soc.*, 1992, **114**, 2277.
- 22 S. Komamine, M. Fujitsuka, and O. Ito, *Phys. Chem. Chem. Phys.*, 1999, **1**, 4745.
- 23 Y. Maeda, R. Sato, T. Wakahara, M. Okamura, T. Akasaka, M. Fujitsuka, O. Ito, K. Kobayashi, S. Nagase, M. Kako, Y. Nakadaira, and E. Horn, *J. Organomet. Chem.*, in press.
- 24 S. Masamune, S. Murakami, and H. Tobita, *J. Am. Chem. Soc.*, 1983, **105**, 7776.
- 25 H. B. Yokelson, A. J. Millevshte, G. R. Gillette, and R. West, *J. Am. Chem. Soc.*, 1987, **109**, 6865.
- 26 R. West, D J. De Young, and K. J. Haller, *J. Am. Chem. Soc.*, 1985, **107**, 4942.
- 27 R. West, *Pure Appl. Chem.*, 1984, **56**, 163.
- 28 S. Masamune, Y. Hanzawa, S. Murakami, T. Bally, and J. F. Blount, *J. Am. Chem. Soc.*, 1982, **104**, 1150.